# Analysis of Springing Effects on Floating Barges in Time Domain by a Fully Coupled Hybrid BEM-FEM

**Yooil Kim*, Yonghwan Kim***
*Seoul National University, Seoul, Korea

## 1. Introduction

Larger and faster ships are far more vulnerable to the fatigue damage because of additional cyclic loading induced by springing excitation in high-frequency range. One of the most critical situations among others is the case of ultra-large container carrier where demand on high speed is utmost with unfavorable low torsional rigidity due to large deck openings. This leads to higher chances of resonant vibration between flexible hull and wave excitation.

Bishop and Price(1979) used generalized concept, where dynamic response of the flexible hull was expressed in terms of its basic natural modes including six rigid body modes. Jensen and Dogliani(1996) carried out a detailed numerical study on nonlinear springing load using a second-order strip theory. Malenica et al.(2003) used a frequency-domain wave Green function method combined with finite element beam model which is able to capture both bending-torsion coupling and warping deformation. In their study, verification through model basin test was carried out with a segmented model composed of 12 separated pontoon-like hulls.

This study concerns ship hydroelasticity problem focusing on springing phenomenon with zero-forward speed under head and oblique sea conditions. A time-domain Rankine panel method is used to represent fluid motion surrounding a flexible vessel, and a finite element method is used for structural response. Structural response is obtained by using a direct integration method, not relying on conventionally used modal superposition method. Expected benefits of using direct integration is easy extension of the numerical method to structural nonlinear problems where small deformation assumption is not valid any longer. To avoid numerical instability related to the added mass term, an iterative implicit method based on the quasi-Newton method is developed. The developed computer program is verified through the comparison with published experimental data, showing good agreement between the two results.

## 2. Theoretical background

### 2.1 Fluid/Structure Domain

In order to obtain the solution of the coupled problem, physical domain is decomposed into two sub-domains, i.e, fluid and structure domains, where the former is handled by a boundary element method while the latter by a finite element method. Velocity field inside fluid domain is obtained by solving boundary integral equation introducing velocity potential, $\phi(\mathbf{x},t)$, satisfying Laplace equation. Linearized free surface boundary condition is to be applied on mean water line level.

The presence of body in fluid domain invokes the linearized body boundary condition imposed on mean body location as Eqn(1). Unlike rigid body case, body boundary condition has to be treated separately for each panel due to the arbitrariness of deformation pattern of flexible hull.

$$\frac{\partial \phi_{d,i}}{\partial n} = \mathbf{V}_i \mathbf{n}_i - \frac{\partial \phi_{I,i}}{\partial n} \quad \text{on} \quad \overline{S}_B \tag{1}$$

,where subscript $i$ means quantity of $i$th panel and $\mathbf{V}$ is velocity of the panel induced by structural deformation. Velocity of each panel can be obtained by interpolating nodal velocity of finite element.

Discrete algebraic equation can be obtained as Eqn(2), where $\boldsymbol{\varphi}$ and $\partial\varphi/\partial n$ indicate disturbed potential vector and its normal derivative both at body and free surface. Bi-quadratic spline function is used to approximate potential distribution on both the body and free surface(Kim et al., 2007a). Submatrix **A** and **R** are influence coefficient sub-matrices. Subscript B and F mean body surface and free surface, respectively.

$$\begin{bmatrix} \mathbf{A}_{BB} & \mathbf{A}_{BF} \\ \mathbf{A}_{FB} & \mathbf{A}_{FF} \end{bmatrix} \begin{bmatrix} \boldsymbol{\varphi}_B \\ \partial \boldsymbol{\varphi}_F / \partial \mathbf{n} \end{bmatrix} = \begin{bmatrix} \mathbf{R}_{BB} & \mathbf{R}_{BF} \\ \mathbf{R}_{FB} & \mathbf{R}_{FF} \end{bmatrix} \begin{bmatrix} \partial \boldsymbol{\varphi}_B / \partial \mathbf{n} \\ \boldsymbol{\varphi}_F \end{bmatrix} \tag{2}$$

The response of flexible structure is calculated by a finite element method. Hull is modeled by 1D beam element which is computationally more efficient than 3D shell model providing sufficient level of accuracy even though the simplification it takes. Timoshenko beam element with Hermitian polynomial is used in order to take into account the effect of shear deformation. The rate of change of twisting angle is added to the conventional 6-DOF beam element to consider warping distorsion, and coupling between bending and torsion is taken into account.

Whole finite element equation is given in Eqn(3) along with its stiffness and mass matrix. Damping is realized in the model by using Rayleigh damping where damping matrix, C, is decomposed into mass proportional one and stiffness proportional one.

$$\begin{aligned} &\mathbf{M}\ddot{\mathbf{d}} + \mathbf{C}\dot{\mathbf{d}} + \mathbf{K}\mathbf{d} = \mathbf{F} \\ &\mathbf{K}_N = \int_V \mathbf{B}^{P\mathrm{T}} \mathbf{D} \mathbf{B}^P dV, \quad \mathbf{M}_N = \int_V \rho \mathbf{N}^{P\mathrm{T}} \mathbf{N}^P dV \end{aligned} \tag{3}$$

### 2.2 Coupling

Strongly coupled approach for partitioned BEM-FEM domain is used in this study. Fixed-point iteration with

relaxation naturally fits to this partitioned approach since there is no further modification of existing program. However, fixed-point iteration is less efficient in terms of computation cost and, moreover, convergence is not always guaranteed. To overcome the limitation of fixed point iteration, quasi-Newton method for coupled BEM-FEM is developed in this study. For this, two Jacobian matrices for both fluid and structure domains need to be constructed prior to the analysis.

Let's assume that both fluid and structure problems, **f** and **s** respectively, can be expressed in concise forms like Eqn(4), where **p** is fluid pressure at panel and **d** is structural deformation at node. All the variables in Eqn(4) are those of current time step, $t+\Delta t$, dropping out the variables of previous time step which is priori known.

$$\begin{aligned}\mathbf{f} &= \mathbf{p} - \mathbf{F}(\dot{\mathbf{d}}, \mathbf{d}) = 0 \\ \mathbf{s} &= \dot{\mathbf{d}} - \mathbf{S}(\mathbf{p}) = 0\end{aligned} \tag{4}$$

Applying Newton method to this coupled two equations, following linear equation can be obtained.

$$\begin{bmatrix} \mathbf{I} & -D_{\dot{\mathbf{d}}}\mathbf{F} \\ -D_{\mathbf{p}}\mathbf{S} & \mathbf{I} \end{bmatrix} \begin{bmatrix} \Delta\mathbf{p} \\ \Delta\dot{\mathbf{d}} \end{bmatrix} = \begin{bmatrix} -\mathbf{f} \\ -\mathbf{s} \end{bmatrix} \tag{5}$$

From Eqn(5), the incremental change of solution, eventually leading to the converged one, can be calculated. Iteration needs to be repeated until there is no more solution change after subsequent iteration. Jacobian matrix in Eqn(5) can be obtained by solving fluid and structure tangent problem after discretization.

Fluid Jacobian matrix, $D_{\dot{\mathbf{d}}}\mathbf{F}$, upper right part of Jacobian matrix, can be obtained by looking into the response of panel pressure with respect to the variation of structural deformation. Eqn(6) shows Bernoulli equation, where all other terms but disturbed potential related ones were dropped out. Under zero forward speed assumption, the discretized version of linear Bernoulli equation can be obtained as shown in Eqn(6).

$$\mathbf{p}_{hyd} = -\rho \frac{\boldsymbol{\varphi}_d^{t+\Delta t} - \boldsymbol{\varphi}_d^{t}}{\Delta t} \tag{6}$$

Disturbed potential of current time step in Eqn(6) is determined by the body boundary condition imposed on the flexible body. By considering body boundary condition and original discretized boundary integral equation, Eqn(6) can be rewritten like Eqn(7), where matrix **B**s are from influence coefficients.

$$\mathbf{p}_{hyd} = -\rho \frac{\mathbf{B}_{11}\left(\dot{\mathbf{d}}_n^P - \frac{\partial \boldsymbol{\varphi}_I}{\partial n}\right) + \mathbf{B}_{12}\boldsymbol{\varphi}_F - \boldsymbol{\varphi}_d^t}{\Delta t} \tag{7}$$

where $\dot{\mathbf{d}}_n^P$ is normal deformation velocity at each panel. Differentiating hydrodynamic pressure with respect to nodal deformation velocity results in Eqn(8).

$$\frac{\partial \mathbf{p}_{hyd}}{\partial \dot{\mathbf{d}}} = \frac{\rho}{\Delta t}\mathbf{B}_{11}\frac{\partial \dot{\mathbf{d}}_n^P}{\partial \dot{\mathbf{d}}^N} = \mathbf{B}\frac{\partial \dot{\mathbf{d}}_n^P}{\partial \dot{\mathbf{d}}^N} \tag{8}$$

where $\dot{\mathbf{d}}^N$ is nodal deformation velocity. If Eqn(8) is rewritten in index notation, Eqn(9) can be obtained. In Eqn(9), index *i* corresponds to panel, index *j* to node.

$$\begin{aligned}\frac{\partial p_{hyd,i}}{\partial \dot{d}_j} &= B_{ik}\frac{\partial \dot{d}_{n,k}^P}{\partial \dot{d}_j^N} = B_{ik}\frac{\partial(\mathbf{n}_k \cdot \dot{\mathbf{d}}_k^P)}{\partial \dot{d}_j^N} = B_{ik}\left(\mathbf{n}_k \cdot \frac{\partial \dot{\mathbf{d}}_k^P}{\partial \dot{d}_j^N}\right) \\ &= B_{ik}\left(\mathbf{n}_k \cdot \frac{\partial\left(\mathbf{N}_k \dot{\mathbf{d}}_{ke}^N\right)}{\partial \dot{d}_j^N}\right) = B_{ik}\left(\mathbf{n}_k \cdot \mathbf{N}_k \frac{\partial\left(\dot{\mathbf{d}}_{ke}^N\right)}{\partial \dot{d}_j^N}\right)\end{aligned} \tag{9}$$

where $\mathbf{n}_k$ is normal vector of k-th panel and $\mathbf{N}_k$ is finite element shape function matrix of k-th panel(Kim et al., 2007b). $\dot{\mathbf{d}}_k^P$ is deformation velocity of k-th panel and $\dot{\mathbf{d}}_{ke}^N$ is element nodal deformation velocity corresponding to the k-th panel.

For complete Jacobian matrix derivation, the contribution of restoring pressure acting on the flexible hull has to be considered as well. Restoring pressure at *i*-th panel is

$$p_{res,i} = -\rho g w_i = -\rho g\left(\mathbf{N}_{3,i}\mathbf{d}_{ie}^N\right) \tag{10}$$

where $\mathbf{N}_{3,i}$ is the 3rd row of the shape function matrix evaluated at i-th panel and $\mathbf{d}_{ie}^N$ is element nodal deformation corresponding to the *i*-th panel. Differentiation of the restoring pressure with respect to nodal deformation velocity yields,

$$\begin{aligned}\frac{\partial p_{res,i}}{\partial \dot{d}_j^N} &= -\rho g\frac{\partial\left(\mathbf{N}_{3,i}\mathbf{d}_{ie}^N\right)}{\partial \dot{d}_j^N} = -\rho g\mathbf{N}_{3,i}\frac{\partial \mathbf{d}_{ie}^N}{\partial \dot{d}_j^N} \\ &= -\rho g\left(\frac{\alpha\Delta t}{\delta}\right)\mathbf{N}_{3,i}\frac{\partial\left(\dot{\mathbf{d}}_{ie}^N\right)}{\partial \dot{d}_j^N}\end{aligned} \tag{11}$$

where index *i* is that of panel, *j* that of node.

Structural Jacobian matrix, $D_{\mathbf{p}}\mathbf{S}$, can be interpreted as the response of nodal deformation velocity with respect to the change of panel pressure acting on the hull. It can be found that nodal deformation velocity can be expressed in terms of excitation force as Eqn(12). This can be obtained without difficulty by handling time discretized FE equation using Newmark-β method.

$$\begin{aligned}\dot{\mathbf{d}} &= \mathbf{M}_1\mathbf{F}(\mathbf{p}) + \mathbf{M}_2 \\ \mathbf{M}_1 &= \left[\frac{\alpha\Delta t}{\delta}\left(\frac{1}{\alpha\Delta t^2}\mathbf{M} + \frac{\delta}{\alpha\Delta t}\mathbf{C} + \mathbf{K}\right)\right]^{-1}\end{aligned} \tag{12}$$

**F**(**p**) is the nodal force vector of hydrodynamic excitation, which is the function of panel pressure. Matrix $\mathbf{M}_2$ contains all the variables of previous time step. Differentiating Eqn(12) by panel pressure will result in,

$$\frac{\partial \dot{\mathbf{d}}}{\partial \mathbf{p}} = \mathbf{M}_1\frac{\partial \mathbf{F}(\mathbf{p})}{\partial \mathbf{p}} \tag{13}$$

Nodal force vector is composed of seven force

components, that is, three translational ones plus three rotational ones including bi-moment. Nodal force is calculated by summing up all panel forces surrounding the *i*-th node after applying some weight factor on it which depends on the location of the panel inside the element. The weight factor is decided by the assumed interpolation function, in this case cubic polynomial function. Eqn(14) shows derivatives of nodal force component, in x, y, z direction, with respect to the panel pressure. Derivatives of vertical and horizontal bending moment as well as torsional moment can be obtained in similar way.

$$
\begin{aligned}
\frac{\partial R_{i,x}}{\partial p_{j+}} &= n_{j+,x}\Delta s_{j+}N_5(\xi_+) \\
\frac{\partial R_{i,x}}{\partial p_{j-}} &= n_{j-,x}\Delta s_{j-}N_6(\xi_-) \\
\frac{\partial R_{i,y}}{\partial p_{j+}} &= n_{j+,y}\Delta s_{j+}N_1(\xi_+) + n_{j+,x}\Delta s_{j+}(-y_+)N_{1,x}(\xi_+) \\
\frac{\partial R_{i,y}}{\partial p_{j-}} &= n_{j-,y}\Delta s_{j-}N_3(\xi_-) + n_{j-,x}\Delta s_{j-}(-y_-)N_{3,x}(\xi_-) \\
\frac{\partial R_{i,z}}{\partial p_{j+}} &= n_{j+,z}\Delta s_{j+}N_1(\xi_+) - n_{j+,x}\Delta s_{j+}(z_+)N_{1,x}(\xi_+) \\
\frac{\partial R_{i,z}}{\partial p_{j-}} &= n_{j-,z}\Delta s_{j-}N_3(\xi_-) - n_{j-,x}\Delta s_{j-}(z_-)N_{3,x}(\xi_-)
\end{aligned}
\qquad (14)
$$

## 3. Analysis Results

To verify the present method, numerical computation is carried out for a flexible model which was experimented by Malenica et al.(2003) and also Remy et al.(2006). Fig.1 shows hydrodynamic panel model used in the numerical analysis.

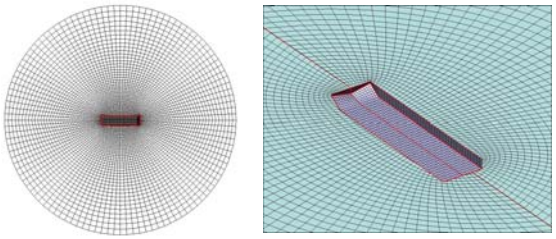

Fig.1 Hydrodynamic panel model
(full model for visibility)

The barge is made of 12 segmented pontoons, and each pontton is 0.19m long, 0.6m wide and 0.25m deep. Overall barge length is 2.445m and draft is 0.12m. Foremost pontoon is slightly modified as shown in Fig.1. 12 segmented pontoons were tied together with two 6mm×50mm steel plates placed side by side on the deck level in Malenica's model (Model A). In Remy's model (Model B), steel plates were replaced by 10mm × 10mm steel rod with same pontoon arrangement. The motion response of the flexible body is compared with a set of experimental data, as shown in Fig.2. Throughout the whole measuring points, agreement between experiment (Malenica et al., 2003) and numerical prediction is fairly good.

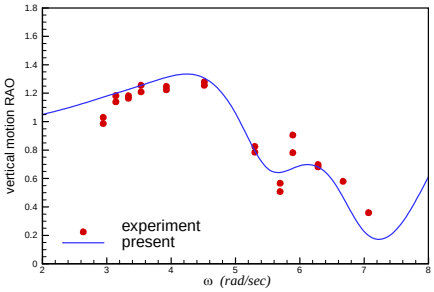


(a) Pt.1

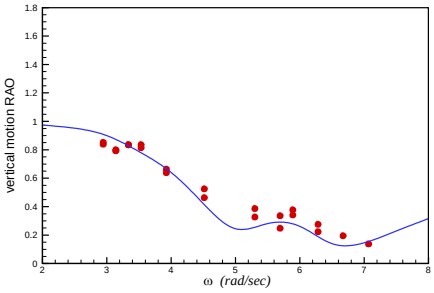


(b) Pt.5

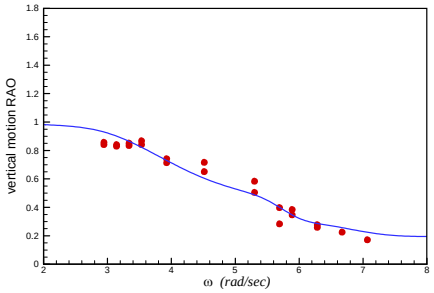


(c) Pt.7

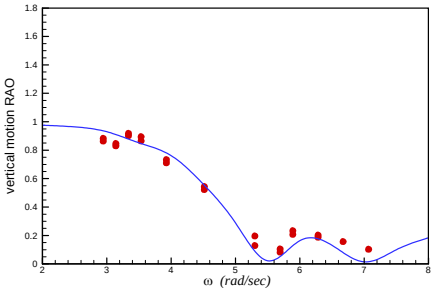


(d) Pt.11

Fig.2 Vertical motion RAOs of flexible body A
(Experimental data from Malenica et al., 2003)

Fig.3 shows comparison of deformed hull under wave excitation. It can be seen that numerical results compare well with those observed in the experiment. This result is the case when wave length is about the size of the floating body with ω= 4.5 rad/sec.

Fig.4 shows the pressure contours when wave frequency is 7.5 rad/sec. It can be seen that hydrodynamic pressure distribution on the flexible body is quite different from that on the rigid body thanks to resonant response in flexible body. It is interesting to note that in this resonant frequency case, unlike long wave case where pressure on rigid body is larger, hydrodynamic pressure on the flexible body is

larger than that on the rigid body.

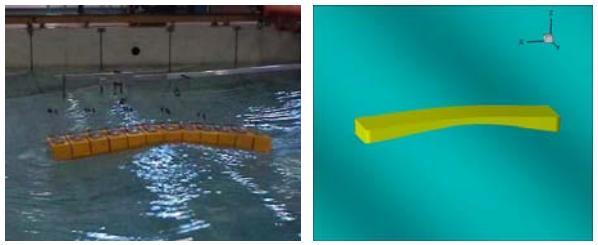

(a) t=T

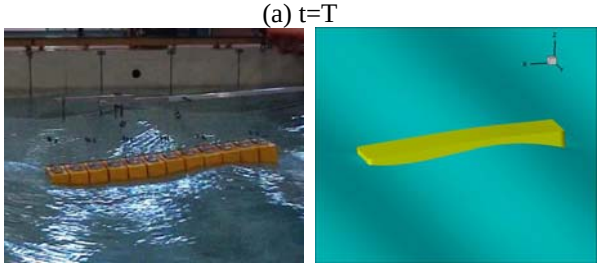

(b) t=T+T/4

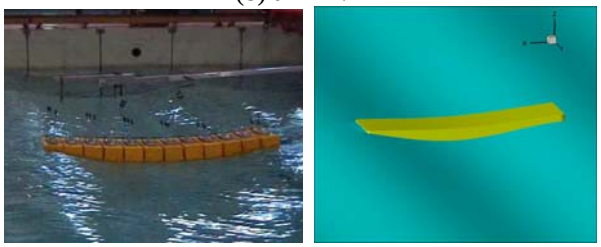

(c) t=T+T/2

Fig.3 Deformation under wave excitation, Model B (Picture from Remy et al., 2006, private communication)

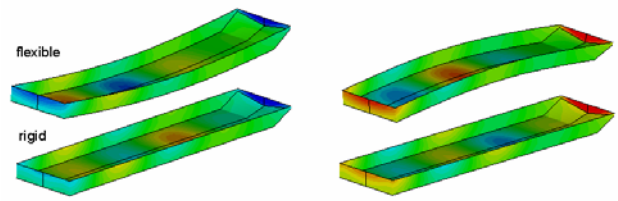


Fig.4 Comparison of instantaneous hydrodynamic pressure between flexible (Model B) and rigid bodies, ω=7.5 rad/sec, left at t= *n*T+T/4, right at t= *n*T+3T/4

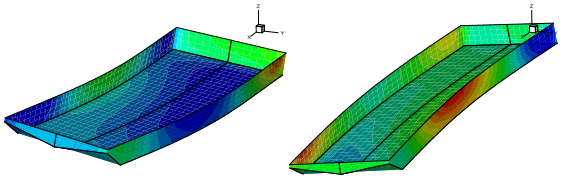

Fig.5 Hydrodynamic pressure on the flexible body(Model B), β=120$^o$, ω=4.0 rad/sec, left at t= *n*T, right at t= *n*T+T/2

Fig.5 shows hydrodynamic pressure distribution on the flexible body when body is exposed to the incoming wave of 120$^o$. It can be seen that the body deforms in such a way that bending and torsion take place at the same time along with rigid body motion making whole picture rather complicated. Unlike head sea case as in Fig.4, high hydrodynamic pressure develops on the side wall near midship due to horizontal bending mode.

## 4. Conclusions

Time domain hydroelasticity program is developed by combining BEM and FEM, each of which is used for fluid and structural domain respectively. Iterative implicit scheme is used for coupling two field equation and quasi Newton method is applied to obtain converged solution. Numerical solution obtained by developed computer program was compared with experimental data with good correspondence between the two. The direct time integration scheme adopted in this study for solving equation of motion is able to overcome incapability of modal superposition method when extension is needed to the problems where geometric nonlinearities of the structural deformation becomes considerable.

## Acknowledgement

Authors appreciate Prof.Molin and Dr.Malenica for their kindness to provide their experimental data. Their data were very helpful for the present study. This study is partially supported by Daewoo Shipbuilding & Marine Engineering and LRET-funded Research Center. Authors thank their support.

## References


- Bishop, R.E.D., and Price, W.G., 1979, *Hydroelasticity of Ships*, Cambridge University Press.
- Jensen, J.J., Dogliani, M., 1996, “Wave-induced ship hull vibrations in stochastic seaways”, Marine Structures 9(3), 353-387.
- Malenica, S, Molin, B, Senjanociv, I, 2003, “Hydroelastic response of a barge to impulsive and non-impulsive wave loads”, Hydroelasticity 2003, Oxford, UK.
- Malenica, S, Senjanovic, I, Tomasevic, S, 2006, “An efficient hydroelastic model for wave induced coupled torsional and horizontal ship vibrations”, 21$^{st}$ IWWWFB, Loughborough, UK.
- Kim, K.H., Kim, Y., Kim, Y., 2007a, “WISH JIP Project Report and User’s Manual”, Project report, Seoul National University.
- Kim, Y., Kim, K.H., Kim, Y., 2007b, “Study on the analysis of ship hydroelasticity by fully coupled hybrid FEM-BEM”, Journal of the Society of Naval Architects of Korea, submitted
- Remy, F., Molin, B., Ledoux, A., 2006, “Experimental and Numerical Study of the Wave Response of a Flexible Barge”, Hydroelasticity in Marine Technology, Wuxi, China.